BIOCHEMISTRY
including biophysical chemistry & molecular biology

Article

pubs.acs.org/biochemistry

Mapping the BH3 Binding Interface of Bcl-x_L, Bcl-2, and Mcl-1 Using Split-Luciferase Reassembly

Sean T. Campbell, Kevin J. Carlson, Carl J. Buchholz, Mark R. Helmers, and Indraneel Ghosh*

Department of Chemistry and Biochemistry, University of Arizona, 1306 East University Boulevard, Tucson, Arizona 85721, United States

Supporting Information

ABSTRACT: The recognition of helical BH3 domains by Bcl-2 homology (BH) receptors plays a central role in apoptosis. The residues that determine specificity or promiscuity in this interactome are difficult to predict from structural and computational data. Using a cell free split-luciferase system, we have generated a 276 pairwise interaction map for 12 alanine mutations at the binding interface for three receptors, Bcl-x_L, Bcl-2, and Mcl-1, and interrogated them against BH3 helices derived from Bad, Bak, Bid, Bik, Bim, Bmf, Hrk, and Puma. This panel, in conjunction with previous structural and functional studies, starts to provide a more comprehensive portrait of this interactome, explains promiscuity, and uncovers surprising details; for example, the Bcl-x_L R139A mutation disrupts binding to all helices but the Bad-BH3 peptide, and Mcl-1 binding is particularly perturbed by only four mutations of the 12 tested (V220A, N260A, R263A, and F319A), while Bcl-x_L and Bcl-2 have a more diverse set of important residues depending on the bound helix.

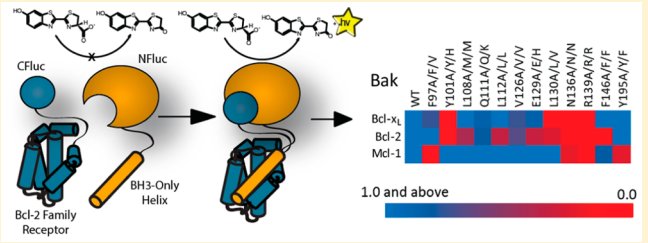

Identifying the physiochemical features necessary for specific protein−protein interactions (PPIs) remains challenging.[1−11] Increased understanding of interfaces is particularly relevant for PPI driven signaling networks and their inhibitors, or for the redesign of interfaces to afford new networks.[12−23] A particularly intriguing system of PPI pairs constitutes proteins from the Bcl-2 family and their ligands, the Bcl-2 homology 3 (BH3)-domain containing proteins. These interactions orchestrate apoptosis, or programmed cell death, and have been the subject of intense study[24−28] to determine binding profiles,[29−32] differential roles in apoptosis,[30,33−40] and mechanisms of mitochondrial pore formation.[35,41−46] However, much is still debated functionally and structurally,[47] such as the specific residues at the interface that impart specificity or promiscuity.[16,17,48−54] Moreover, the role of the Bcl-2 family in triggering or preventing apoptosis has rendered this class of interactions as potential therapeutic targets implicated in disease.[24,55−60] There has been a significant body of work focused on the generation of small molecule mimetics,[61−73] peptides,[16,74−76] miniature proteins,[20,77,78] stabilized helices,[79−88] and foldamers,[89−96] with a variety of specificities that target this interface. Herein, we focus on the residues at the interface that can potentially dictate specificity or promiscuity within this interactome.

The Bcl-2 protein family encompasses two major classes: Bcl-2 homologues which contain 2−4 of the helical "Bcl-2 homology" or "BH" domains and are similar to the titular Bcl-2, and BH3-only proteins, which contain only the Bcl-2 homology 3 domain.[28] The Bcl-2 family is further subdivided into anti-apoptotic (such as Bcl-2, Bcl-x_L, and Mcl-1) and pro-apoptotic (such as Bak and Bax) groups on a functional basis. Structurally, the Bcl-2 receptor family forms a cleft, primarily comprising helices from the BH 1, 2, and 3 domains, which then serve to cradle various BH3 helices (Figure 1).[28] Several NMR and crystal structures of these proteins have been solved[32,41,46,50,51,66,93,97−104] and provide a structural framework for discussing the potential role of specific residues at the interface.

An understanding of binding determinants is relevant for the selective activation or inhibition of these interactions from a signaling and therapeutic standpoint.[16,48,66,101,104] However, the molecular interactions that dictate BH3 peptide helices binding to the BCl-2 family receptors are not well understood as many BH3-only peptides bind to several receptors and vice versa.[29−32] The few systematic experimental studies to date have focused upon mutational analysis of residues that dictate specificity and affinity of the helical BH3 domains.[16,50−54] A few studies have interrogated the residues within the receptor cleft,[17,48,49] however not systematic alanine mutations. Of note, Keating and co-workers covaried multiple residues in order to enhance selectivity for specific BH3 helices.[17] Computational studies have also probed this interface,[105,106] but they require experimental validation.

Determining the explicit role of individual residues in the receptor cleft that contribute to the recognition of their cognate BH3 helices is necessary for deconvoluting the factors that govern specificity and promiscuity. Moreover, such results will

Received: December 9, 2014
Revised: March 23, 2015
Published: April 6, 2015

DOI: 10.1021/bi501505y
Biochemistry 2015, 54, 2632−2643

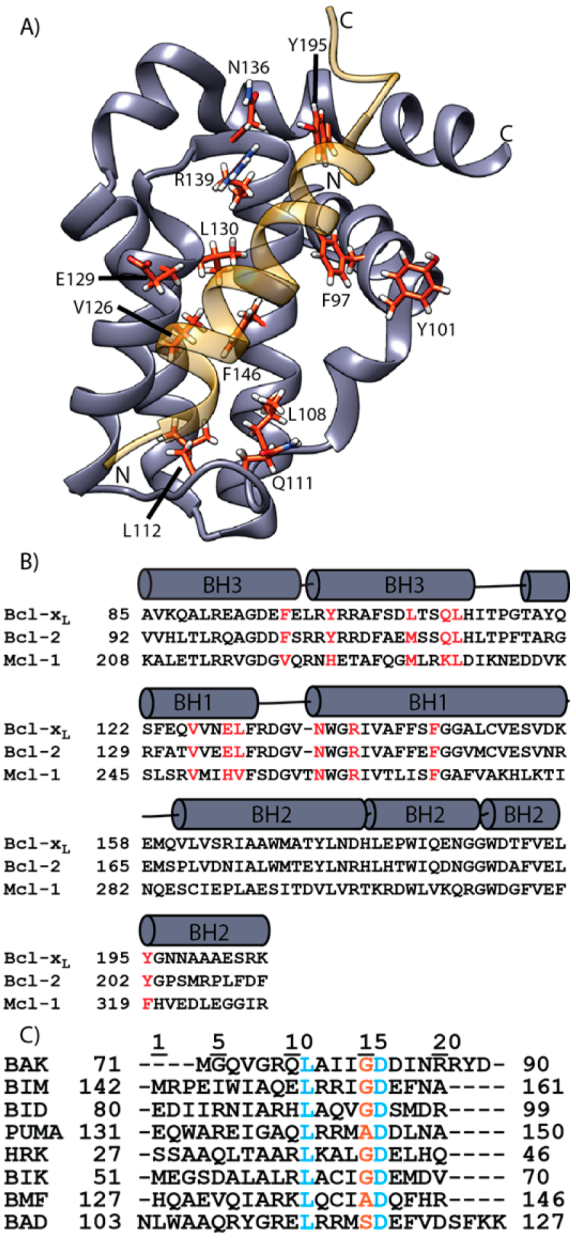

Figure 1. (A) Structure of Bcl-x_L (gray, residues 85−205) bound to Bad (gold, residues 103−127), PDBID 1G5J. All residues mutated in this study are shown in red. (B) Alignment of Bcl-x_L, Bcl-2, and Mcl-1. Residues shown correspond to the portion of the structure shown in A. Residues mutated to alanine in this study are shown in red. (C) Aligned sequences for the eight BH3 domain helices used in this study. The conserved residues, L11 and D16, are shown in blue, and the partially conserved residue 15 is shown in orange.

help test and refine predictive computational methods, aid in the design of inhibitors, and provide starting points for redesigning these interfaces to provide orthogonal helix/receptor pairs for the potential design of new networks,[21] as well as for the design of edgetic mutants (where a molecule with a complex interaction network is reduced by a single interaction, or "edge" of the network) for the purpose of elucidating the Bcl-2/BH3 network.[15,17] The individual interrogation of a large number of receptor/helix pairs is experimentally demanding, yet necessary for understanding these interfaces. Thus, in order to tackle this problem, we adopted a cell-free split-luciferase system.[107−110]

We have previously validated the split-luciferase approach with known helix-receptor binding partners and also have shown that it is useful for demonstrating the specificity of small molecule and peptide inhibitors.[68] The cell-free split luciferase method exists in between classic *in vivo* methods,[111,112] often complicated by indirect readouts,[113] and classical biochemical approaches. In order to probe the BH3 interactome, we first validated several known interactions and subsequently created 12 alanine mutants at each of the binding interfaces for Bcl-x_L, Bcl-2, and Mcl-1 (Figure 1A,B) and interrogated them against BH3 helices derived from Bid, Bim, Bad, Bik, Bmf, Bak, Hrk, and Puma (Figure 1C), to provide a map of 23 protein partnerships comprising 276 pairwise interactions (Mcl-1:Bad data are not reported, as the binding affinity of the wild-type complex is too low to provide accurate values in this study[29,31]). This study goes toward explaining promiscuity and the role of specific residues in this important and widely studied interactome.

MATERIALS AND METHODS

Plasmids and Mutagenesis. For the BH3-only peptides (Bad, Bak, Bik, Bim, Bid, Bmf, Hrk, and Puma), all sequences from *Homo sapiens* (Figure 1C) were coupled on the N-terminus of the N-terminal half of *Photinus pyralis* (firefly) luciferase (NF) via a glycine/serine linker in the pcDNA 3.1 vector. Bcl-x_L, Bcl-2, and Mcl-1 (all *H. sapiens*) were linked to the C-terminus of the C-terminal half of firefly luciferase (CF) in the pEF6 vector. Site-directed mutagenesis was done through the use of PfuUltra or Kapa HiFi enzymes. Twelve mutants of Bcl-x_L (F97A, Y101A, L108A, Q111A, L112A, V126A, E129A, L130A, N136A, R139A, F146A, Y195A), a single mutant each of Puma and Hrk (A15S, and G15S, respectively), three mutants of Bim (G15A, G15S, and D16A), and two mutants of Bak (R9A and L11A) were generated in this manner. Additionally, mutations homologous to those made in Bcl-x_L were made in Cf-Bcl-2 (F104A, Y108A, M115A, Q118A, L119A, V133A, E136A, L137A, N143A, R146A, F153A, Y202A) and CF-Mcl-1 as well (V220A, H224A, M231A, K234A, L235A, V249A, H252A, V253A, N260A, R263A, F270A, F319A). All sequences were verified with dideoxynucleotide sequencing.

mRNA Synthesis and Split-Luciferase Assay. PCR fragments of the luciferase-coupled constructs were created with appropriate primers. For the CF constructs, the forward primer contained the T7 and Kozak consensus sequences. For NF constructs, these sequences were already contained in the host plasmid. A stabilizing stem loop was included in the reverse primer for all constructs. RNA was generated from these products using the RiboMAX large-scale RNA production system. RNA size and purity were confirmed with gel electrophoresis, and concentrations were taken by absorption at 260 nm. A total of 0.1 pmol of mRNA for each construct RNA for Bcl-x_L reactions or 1 pmol of each for Bcl-2 and Mcl-1 reactions was added to a total volume of 24 μL of reticulocyte lysate and incubated at 30 °C for 1.5 h. Following translation, 40 μL of L-Glo luciferase assay reagent was added to a 10 μL aliquot of translation reaction, and light emission was monitored immediately after mixing with a Turner Biosystems luminometer with 10 s integration time. All reported values are the average of at least two repeats.

Expression and Purification. The wild-type and R139A mutant Bcl-x_L were cloned into the pET 15b vector for expression in *Escherichia coli*. While the full-length construct

DOI: 10.1021/bi501505y
Biochemistry 2015, 54, 2632−2643

was used in *in vitro* studies, a C-terminally truncated version (Bcl-x_L-209 and Bcl-x_L-209-R139A, AA 1−209) was used for expression with an N-terminal hexahistidine tag separated from the Bcl-x_L sequence with thrombin and TEV cleavage sequences. Cells were grown in media containing ampicillin, and protein expression was induced with 1 mM IPTG. Cells were lysed with sonication, and expressed protein was purified via metal-chelate chromatography with Ni-NTA agarose beads. The proteins were further purified via FPLC on a Superdex 75 16/60 HiLoad column into TBS buffer (10 mM Tris, 140 mM NaCl, pH 7.6) and subsequently concentrated. Concentrations were determined from absorption at 280 nm.

Peptide Synthesis. The Bad-BH3 peptide was synthesized via solid-phase peptide synthesis using FMOC chemistry on a Rink amide resin. Peptide was purified via HPLC and confirmed by mass spectrometry. Bad-BH3 sequence: NLWAAQRYGRELRRMSDEFVDSFKK.

ITC Analysis of Bad-BH3 Binding. Expressed proteins were extensively buffer exchanged and diluted in TBS buffer to between 16 and 19 μM. Bad-BH3 peptide was dissolved and diluted in TBS buffer to a concentration between 160 and 190 μM. All stocks were degassed with a ThermoVac apparatus, and approximately 1.4 mL of protein and 0.3 mL of peptide stocks were added to the ITC cell and needle, respectively. Peptide was injected in three 2 μL injections over 4 s each followed by 20 eight 8 μL injections over 16 s each, with a 6 min interval between injections at a cell temperature of 26 °C and reference power of 25 μcal/s. The cell was continuously stirred at 300 rpm. Background was taken by injecting peptide into buffer and buffer into protein, and the resulting traces were subtracted from the sample traces. Residual mechanical effects were subtracted by averaging the last three points and subtracting the resulting value from all points, and the first four injections were removed from all traces before fitting. Data were fitted with the Origin software with a single-site binding model. K_A, ΔH, and N were calculated by the software from the fit and used to calculate the values of K_D,ΔG, and $T\Delta S$.

RESULTS

Choice of Residues for Alanine Scanning. We chose three Bcl-2 family "receptors", Bcl-x_L, Bcl-2, and Mcl-1, for determining their residue specific selectivity for BH3 helices. Bcl-x_L and Bcl-2 were chosen as they share the highest sequence similarity, while Mcl-1 was chosen as it is the most distant (Figure 1B). Available crystal and NMR structures were inspected for side chains that lie within 4 Å of every BH3 helix residue at the interface (Figure 2A). On the basis of this analysis, 12 positions within the cleft were determined to make potential contacts (≤2.5 Å) with several helices across the different receptors and were chosen for further mutagenesis (Supporting Information, Table S1). The residues included F97, Y101, L108, Q111, L112, V126, E129, L130, R139, F146, and Y195 in Bcl-x_L, and the homologous residues in Bcl-2 and Mcl-1 (Figure 1A,B; for ease of notation, when referring to multiple receptors the numbering from Bcl-x_L has been used). N136 was additionally chosen for close contact with Bim, as well as its total conservation across the Bcl-2 family receptors (Figure 1B). We next turned toward developing a method to analyze the desired interactions using a split-luciferase methodology.

The split-luciferase system involves the conditional reconstitution of firefly luciferase and concomitant luminescence when attached protein domains interact (Figure 2B). The split-

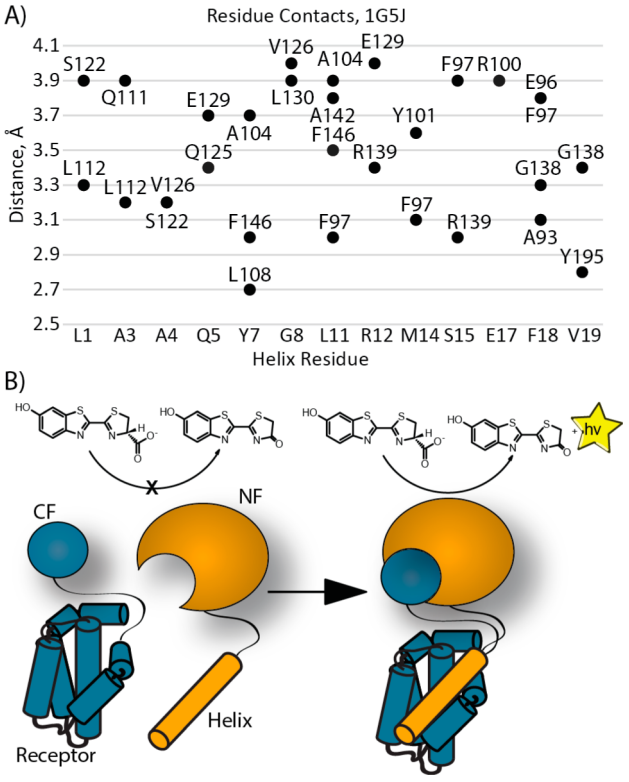

Figure 2. (A) Distances between residues of Bad (lower axis) and Bcl-x_L (filled circles) for a sample structure, 1G5J. Bad residues with no contacts within 4 Å are omitted. (B) Schematic representation of the in vitro cell free split-luciferase reassembly method.

luciferase system is dependent on the binding constants of the conjugated domains,[108] and we have previously demonstrated that the cell free split-luciferase system provides a viable method for rapidly interrogating helix/receptor interactions and their inhibitors.[68,86,107] This method has been shown to faithfully recapitulate binding specificities of helix/receptor type interactions, such as p53/hDM2, p300/Hif1α, and the Bcl-2 family in cell lysates that perhaps provide better approximation of a cellular environment.[68]

In order to validate this methodology several residues from the helices that have been previously mutated in the literature (Bak R9A, Bak L11A,[51] Bim G15A, and Bim D16A[52]) were first tested in our system against Bcl-x_L. The results from this proof of principle experiment verified that the cell-free split-luciferase method strongly correlates with data obtained using standard biophysical methods with purified proteins and peptides (Supporting Information, Table S2 and Supporting Information, Figure S1).

To build the panel of alanine mutants, the Bcl-x_L, Bcl-2, and Mcl-1 receptors were conjugated to the c-terminal fragment of firefly luciferase (CF), to produce CF-Bcl-x_L, CF-Bcl-2, and CF-Mcl-1, while the panel of BH3 conjugates, containing the helical BH3 domains of Bid, Bim, Bad, Bik, Bmf, Bak, Hrk, and Puma, were conjugated to the N-terminal fragment of luciferase (NF) (Supporting Information, Table S3). Once the panel of alanine mutants was created, mRNA stocks of all conjugates were synthesized and translated at equivalent concentrations in reticulocyte lysate followed by addition of the luciferase substrate, luciferin, and measurement of luminescence. We separately interrogated all 288 receptor mutant/BH3 helix pairs, resulting in binding profiles which were internally

DOI: 10.1021/bi501505y
Biochemistry 2015, 54, 2632−2643

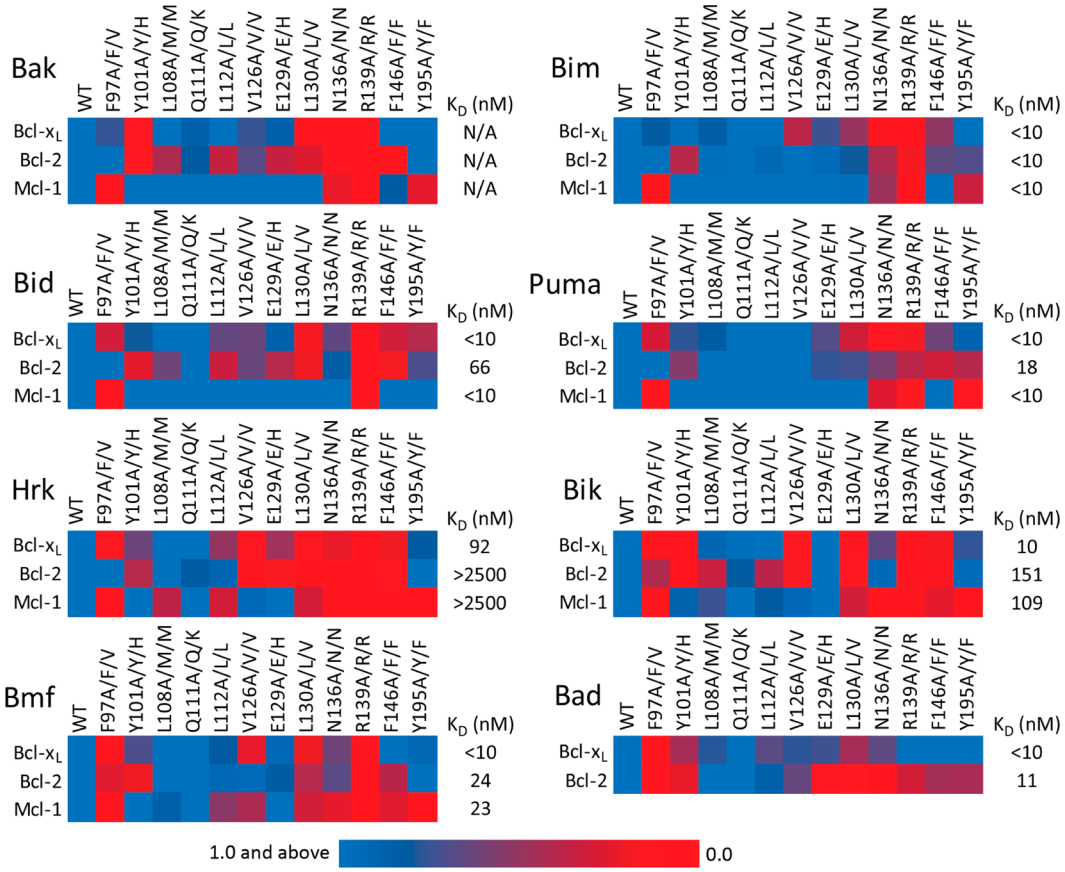

Figure 3. Heat maps of luminescence readings for all 12 receptor mutants with all eight tested BH3 domains. Rows show the mutations using the Bcl-x_L numbering scheme, for example, F97A, followed by the analogous residue in Bcl-2 and Mcl-1, respectively. Luminescence readings for each receptor−helix pair are normalized against the wild type receptor signal which is assigned a value of 1 (green) and a complete lack of binding upon mutation is assigned a value of 0 (red). In this analysis, normalized values when >1 were assigned a value of 1. The Mcl-1 values for Bad binding are not included as that complex shows significantly reduced wild-type binding compared to all other partnerships. The reported K_D's from Certo et al.[31] are provided as a frame of reference.

normalized with the 24 relevant wild type (WT) receptor/helix pairs to directly compare the relative importance of residues at the interface in cell lysates (Figure 3, Supporting Tables S4−9 and Figure S2). In certain instances, mutations resulted in higher signal or values above 1, which may imply tighter binding, which we will explore in due course. For the current study focused upon understanding positive determinants of binding, the values above 1 (wild type) are treated as equivalent to wild type in Figure 3. We also note that the numbers we report are from experiments in cell-like environments which may provide potential off-target macromolecular partnerships that may also influence the results herein.

Analysis of Results. The Bcl-2 homology family of receptors share high similarity with regard to the residues at the interface (Figure 1B), while the BH3 helices share only two conserved residues, L11 and D16, though there is a constellation of hydrophobic residues at positions 7, 14, and 18, corresponding to the residues buried upon binding (Figure 1C). The residue specific basis of high affinity yet promiscuous binding by these receptors[29−32] toward BH3 helices is not well understood. We reasoned that this promiscuity toward BH3 helices may come about through several mechanisms, where (a) a few conserved positions on each receptor, or conserved "hot-spots"[1] confer most of the binding energy (≥1 kcal/residue) for a particular helix; (b) nonconserved hot-spot residues confer most of the binding energy for a particular helix; or (c) numerous rather than a few residues on each receptor contribute to the binding, and the binding energy is distributed across the interface. In this study where concentrations, and thus direct thermodynamic data, are challenging to measure, we classified residues as important or "hot-spots" if their mutation to alanine resulted in ≥50% reduction in binding compared to WT, as measured by a decrease in luminescence in the split-luciferase assay (Figure 3). We observed that either one or the other of the first two possible mechanisms predominate, which likely accounts for the promiscuity of these receptors. For instance, Bak recognition by Bcl-x_L requires the hot-spot residues Y101, L130, N136, and R139. In contrast, Bim recognition by Bcl-x_L requires a different set of residues, V126, N136, and R139, and not Y101 and L130. On the other hand, if we compare two receptors, other differences exist. For example, while Bcl-2 and Bcl-x_L share most hot-spot residues for Bak, Bcl-2 binding is greatly perturbed by the removal of F153, while for Bcl-x_L the homologous F146 is unimportant. We attempt to pictorially capture these observations in Figure 4, where the residues important for the formation of a complex, either helix centric (across a row) or receptor centric (down a column), are highlighted for several complexes. These hot-spot residues are not completely conserved between complexes, though most complexes arise from a small number of hot-spot residues (2−5 residues each).

DOI: 10.1021/bi501505y
Biochemistry 2015, 54, 2632−2643

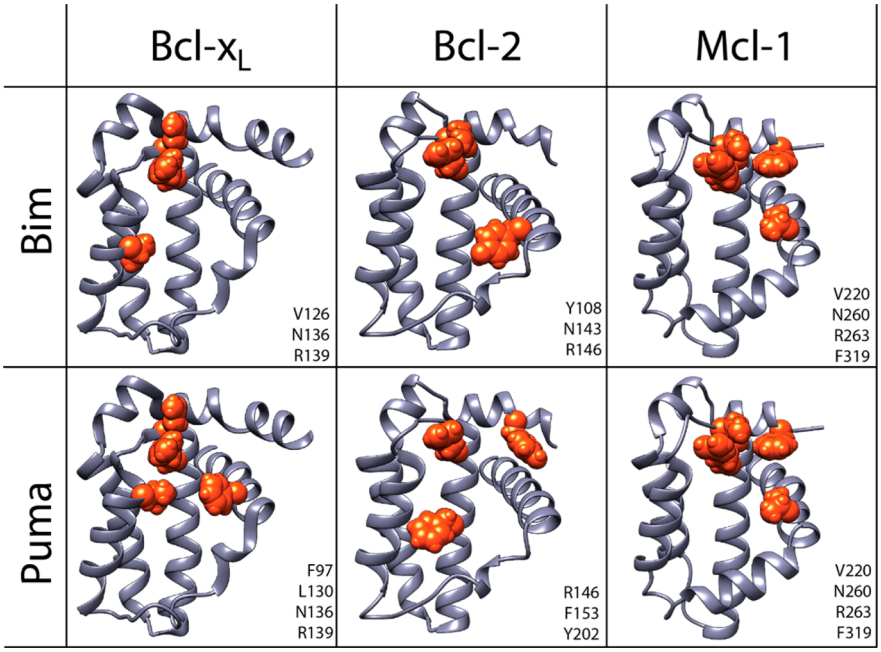

Figure 4. Examples of binding interfaces across different receptor and helix pairs. Residues shown and listed are those when mutated to alanine result in a 50% or greater reduction in signal for the given helix/receptor pair. All images of each receptor are from a single structure (Bcl-x_L from 3PL7, Bcl-2 from 2XA0, Mcl-1 from 3PK1) and may not be representative of the receptor's structure bound to the given helix, which are only available for Bcl-x_L:Puma (2M04), Bcl-x_L:Bim (3FDL), and Mcl-1:Bim (2PQK).

We next focused upon the few "more conserved" hot-spot residues in this panel (Figure 3). The most striking residue that we discovered, R139, is necessary for binding to all helices for both Bcl-2 and Mcl-1, and seven out of eight helices for Bcl-x_L, though surprisingly it is not necessary for Bcl-x_L to bind Bad. F97 in Bcl-x_L is necessary for binding to all helices except for Bim and Bak, while it is only important for four of the eight helices for Bcl-2 (Bid, Bad, Hrk, and Bik). Other hot-spot residues are L130, which is necessary for Bcl-x_L binding to all helices except Bim and necessary for Bcl-2 binding to all helices except Bim and Puma, as well as Y101 which is critical to Bik and Bak binding for both Bcl-2 and Bcl-x_L. The overall binding profile for the more distant Mcl-1 shows less diversity relative to the other two tested members. Four positions (V220, N260, R263, and F319 in Mcl-1) are the only residues important for binding to most helices tested except Hrk and Bmf, which are perturbed by additional mutations.

Interestingly, the BH3 helix Hrk shows a more distributed binding profile in general, as binding to all three receptors is greatly perturbed by at least seven different mutations, the most for any helix. This binding profile may potentially be a result of a lower overall binding affinity of the Hrk peptide.[31] This is possibly consistent with a correlation (R^2 = 0.6) between measured affinities and the number of hot-spot residues determined in this study (see Supporting Information S9–S11 for a more complete discussion).

Overall, our results are most consistent with a nonconserved hot-spot model, where each complex has a different constellation of important or "hot-spot" residues, sharing only a few commonalities with other complexes (Figure 4). The ability of the receptors to offer alternative residues for recognizing different BH3 helices is likely responsible for their promiscuity.

The results of this study were also compared to the computational alanine scan results produced by the Robetta[114,115] and Rosetta[116] programs for available Bcl-x_L:BH3 complexes. Correlation coefficients between the experimental results, albeit relative signal rather than dissociation constant, and computed values varied considerably among structures (Supporting Information, S12–S14). The correlation, R^2, of our experimental data vs Robetta/Rosetta predictions is 0.37/0.04 for 1G5J, 0.02/0.29 for 1BXL, and 0.31/0.13 for 3FDL, respectively. This lack of correlation is possibly a result of potential structural flexibility in the Bcl-2/BH3 family complexes, making computations more challenging.[100,104,105] The correlations seen from this study are consistent with those seen in similar modeling of the Bcl-2 family with Robetta.[53,54] Only the Bcl-x_L:Bad (IG5J) structure displayed correlations of 0.37, which is comparable to those reported by Kleanthous, Baker and co-workers for colicin endonucleases,[117,118] in an alanine scanning study. In addition, the results of this work were also compared to the molecular dynamics simulations determined by Moroy et al.;[106] however, similar low correlations were observed. This analysis together with the lack of availability of structures for most of the helix/receptor interactions, most notably all Bcl-2 complexes tested, suggests experimental approaches remain necessary for interrogating this interactome.

The R139A Mutant. One of the most striking outcomes of this study is the R139A mutation in the receptors, which strongly decreases binding for every pair except for Bcl-x_L:Bad. When the available Bcl-x_L structures are surveyed, only residues 12, 15, and 16 of the helices have side chains within 3 Å of R139. Two of these positions, 12 and 16, are identical in Puma, Bad, and Bim, despite the differences in binding (Figure 5A,B). We hypothesized that it is possible that the serine at position 15 of Bad, a known site of phosphorylation in vivo,[119−121] is the determining factor in binding. Specifically, it has been shown that phosphorylation at this position disrupts Bcl-x_L binding, promoting cell survival,[120] and the importance of this position

DOI: 10.1021/bi501505y
Biochemistry 2015, 54, 2632−2643

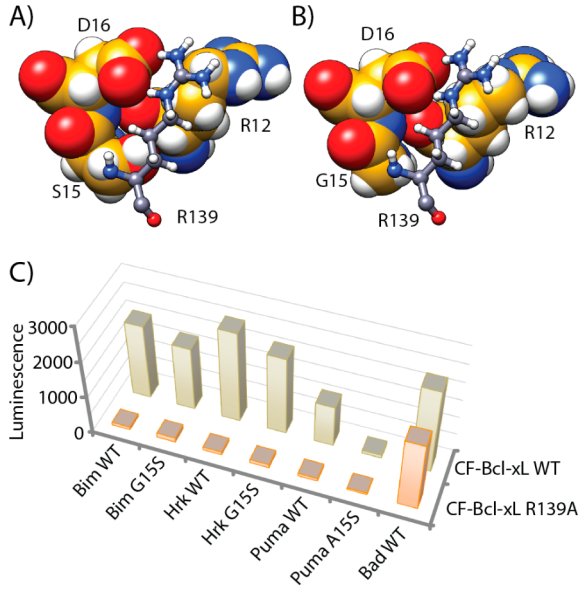

Figure 5. (A) Bcl-x_L R139 (blue, ball and stick) and surrounding Bad residues R12, S15, and D16 (gold, spheres) (2BZW). (B) Bcl-x_L R139 (blue, ball and stick) and surrounding Bim residues R12, G15, and D16 (gold, spheres) (3FDL). (C) Comparison of binding of Bim, Hrk, and Puma mutants and Bad WT to Bcl-x_L WT and Bcl-x_L R139A. Residues at position 15 of the three BH3 peptides were mutated to serine for comparison with Bad WT.

has been supported by the Keating laboratory, who found that mutation of Bad S15 to any residue other than alanine or glycine led to a loss in binding to Bcl-x_L.[53] Thus, it is possible that the serine in this position offers binding affinity.

To test this, the Bim and Puma peptides were mutated to serine at this position, along with Hrk which varies at position 12 but maintains binding to the wild-type Bcl-x_L. However, these mutants did not rescue binding to the R139A mutated receptor (Figure 5C). As a result, the change in binding at this position upon phosphorylation of the S15 residue may be of interest and will be addressed in the future with *in vitro* methods and phosphorylated peptides.

Interestingly, R139A has previously been reported as a knockout mutant.[49,51] Thus, the ability of the R139A mutant to bind Bad was unexpected, but not in disagreement with the previous functional studies, as binding solely to Bad may not be sufficient to preserve the anti-apoptotic ability tested.[29−32] Computational predictions from Robetta and Rosetta showed either no effect upon mutation or a very large negative effect, depending on whether the structure was determined by NMR (no effect) or crystallography (large effect). Moroy et al. have found similar results with the two starting structures but suggested that the NMR results are possibly anomalous and that the R139 residue is important for binding Bad.[106] Given the unique properties of R139A, we set out to biophysically characterize this interaction and to also rule out any potential artifacts stemming from the split-luciferase methodology.

In Vitro Analysis of the Bcl-x_L R139A/Bad Complex. The Bcl-x_L wild-type and R139A mutant were expressed in *E. coli* and purified (Supporting Information Figures S14 and S15). Circular dichroism (CD)[122,123] was used to determine the secondary structure of the mutant. The CD spectra from the wild type and the mutant were very similar (Supporting Information Figure S16) and agree with previous studies of wild-type structures,[104,124,125] showing the R139A mutant to be a helical protein.

In order to test the binding of the mutant to the Bad-BH3 helix, the 25 residue Bad peptide was synthesized for ITC studies (Supporting Figures S17 and S18). The Bad peptide was separately titrated into Bcl-x_L wild type and the R139A protein and the resulting thermodynamic data were compared (Figure 6 and Table 1). These experiments, with certain caveats

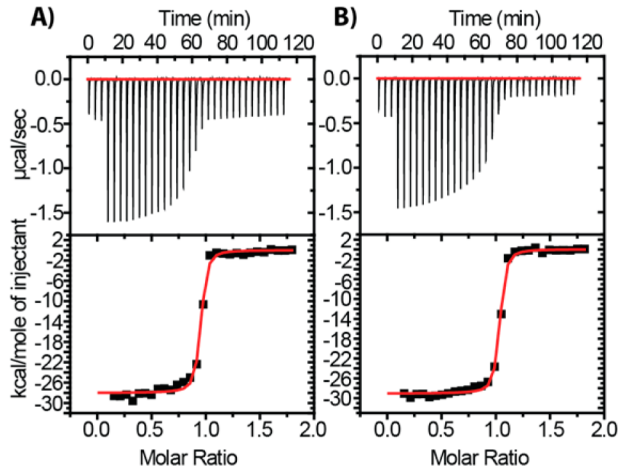

Figure 6. ITC traces for binding of the Bad-BH3 peptide to (A) Bcl-x_L WT and (B) Bcl-x_L R139A. Top panels: raw calorimetric data. Bottom panels: ΔH values obtained from integration of the calorimetric peaks after background subtraction. The red line is the best fit calculated by the Origin software and used to determine the values in Table 1.

Table 1. Biophysical Data for the Binding of Bcl-x_L WT and R139A to Bad from ITC

binding to Bad-BH3	Bcl-x_L WT	Bcl-x_L R139A
K_D (nM)	12.50 ± 2.87	11.14 ± 2.01
ΔH (kcal/mol)	−28.01 ± 0.23	−29.05 ± 0.17
$T\Delta S$ (kcal/mol)	−17.19	−18.16
ΔG (kcal/mol)	−10.82	−10.89

stemming from the high affinities,[31,126] show that both proteins bind to Bad with comparable low nanomolar dissociation constants, K_D, and that the ΔH value for the binding of Bad to the R139A mutant is very similar to wild-type, both of which are consistent with our split-luciferase assay results (Table 1). Thus, the R139A mutant of Bcl-x_L in the context of Bad is an interesting biophysical outlier and may have biological consequences that will be pursued in due course.

DISCUSSION

In order to provide one of the first complementary analysis of the receptor pocket for the BH3 helices, we compared our results to the limited number of systematic mutagenesis studies of the helices. We compared our results to the results from helix mutational data from the Fesik (Bcl-x_L:Bak),[51] Gellman (Bcl-x_L:Bim and Mcl-1:Bim),[52] and Keating laboratories (Bcl-x_L:Bim and Mcl-1:Bim)[16] (Figure 7), providing a complementary view of the helix/receptor interface.

In the case of the Bak alanine scan undertaken by Fesik and co-workers,[51] similar effects seen when contacting residues from the helix and receptor (Bcl-x_L) are compared (Figure 7A). For instance, when the conserved L11 residue of Bak (numbering from Figure 1C) is mutated, binding was shown

DOI: 10.1021/bi501505y
Biochemistry 2015, 54, 2632−2643

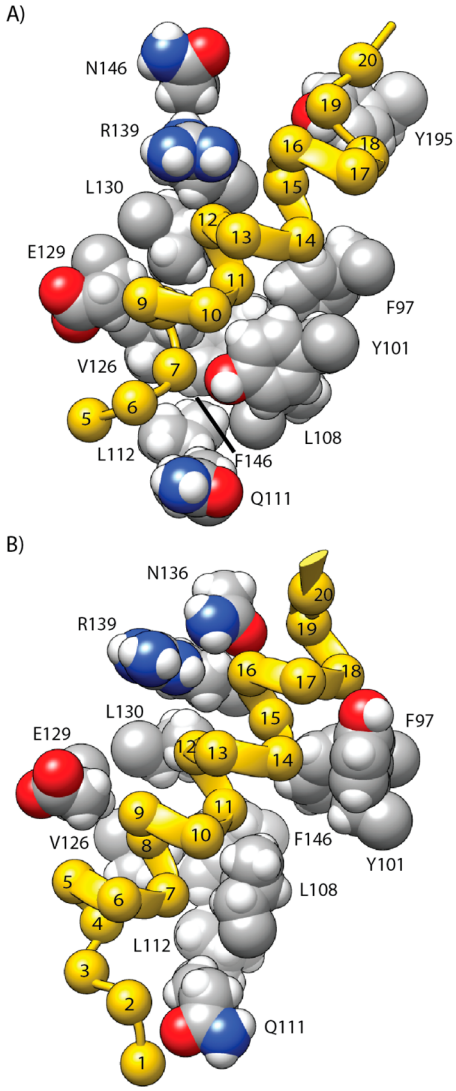

Helix: Bak Mutations[a]	Receptor: Bcl-x_L Contacts ≤ 3 Å[b]
V7 (44)	Y101 (0.1), L112 (1.0), V126 (0.7), E129 (0.9)
G8 (ND)	V126 (0.7), E129 (0.9), L130 (0.1)
R9 (9.7)	E129 (0.9)
Q10 (ND)	Y101 (0.1)
L11 (790)	F97 (0.8), Y101 (0.1), L108 (1.0), V126 (0.8), L130 (0.1)
A12 (ND)	No contacts
I13 (2.9)	No contacts
I14 (50)	F97 (0.8), Y101 (0.1)
G15 (1.5)	No contacts
D16 (122)	N136[c] (0.1), R139[c] (0.0)
D17 (0.4)	No contacts
I18 (275)	Y195 (1.2)

Helix: Bim Mutations[d]	Receptor: Bcl-x_L Contacts ≤ 3Å[e]
I7 (All except D/E) (6.8)	L108 (0.8), L112 (1.1), V126 (0.4)
A8 (A/G) (1.0)	V126A (0.4), E129 (0.7)
Q9 (ND) (1.5)	No contacts
E10 (All except ILFYP) (0.9)	L108 (0.8)
L11 (L) (>90)	F97(0.8), L108 (0.8), V126 (0.4), L130 (0.6)
R12 (K/R/Q/A) (2.8)	E129 (0.7), L130 (0.6), R139 (0.1)
R13 (ND) (5.4)	No contacts
I14 (All) (0.3)	F97 (0.8), Y101 (1.0), L108 (0.8)
G15 (A/G) (0.3)	F97 (0.8)
D16 (D) (33)	N136 (0.1), R139 (0.1)
E17 (D/E) (2.0)	Y101A (1.0)
F18 (F/Y) (>90)	F97 (0.8), Y101 (1.0)

Figure 7. Structure of helix (yellow) binding to the mutated residues in (A) Bcl-x_L:Bak (1BXL) and (B) Bcl-x_L:Bim (3FDL) and comparison to previous scan data for each complex. 3FDL does not contain the Y195 residue. [a]Bak alanine scan from ref 51. Fold differences in binding to Bcl-x_L as compared to wild-type are shown in parentheses. Values from residues that cause a 10-fold or greater reduction in binding shown in red. [b]Bcl-x_L side chains that come within 3 Å of the specified helix residue from Bak. Relative binding from this paper (Figure 3) as compared to wild-type Bak (1.0) shown in parentheses. "Hot-spot" residue values shown in red. [c]Residues that are not within 3 Å in 1BXL but are considered important for binding. [d]Mutations to the Bim helix from refs 16 and 52. Residue substitutions that maintain significant binding to Bcl-x_L in 16 and fold differences in binding to Bcl-x_L as compared to wild-type Bim in 52 are shown in parentheses. Substitutions for residues that tolerate four or fewer other residues in ref 16 and fold differences for alanine mutants showing 10-fold or greater reduction in binding from ref 52 shown in red. [e]Bcl-x_L side chains that come within 3 Å of the specified helix residue from Bim. Relative binding from this paper (Figure 3) as compared to wild-type Bim (1.0) shown in parentheses. "Hot spot" residue values shown in red.

to decrease by 790 fold. Mutation of most residues on the Bcl-x_L receptor with side chain atoms within 3 Å of L11 (F97, Y101, L108, V126, and L130) results in a concomitant decrease in binding to Bak. The receptor residues form a hydrophobic pocket which cradles the L11 residue, and this observation is largely replicated in the patterns of binding for other helices. The residues that are most perturbed through mutation and likely important for this pocket (Y101 and L130) are not predictable *a priori*. When we consider D16, the Bcl-x_L:Bak structure does not show any receptor residues within 3 Å; however, other structures of Bcl-x_L bound to Bim and Bad show proximity between the D16 residue and the conserved N136 and R139 residues of Bcl-x_L, which likely explains the sharp decrease in binding when any of the three residues are mutated.

Similarly, when we compare results of previous SPOT analysis, which comprises mutagenesis of each position on Bim to 18 proteogenic amino acids on the Bim-BH3 peptide carried out by Keating and co-workers[16] to our data set (Figure 7B), we also observe concordance. For instance, the A8 residue of Bim was resistant to mutation in the case of binding to Bcl-x_L. According to crystal structures of Bim bound to Bcl-x_L, the A8 residue lies within 3 Å of the side chains of V126 and E129, and both reduced binding if mutated, though V126 was more important.

Interestingly, for Bim F18, which both Keating and Gellman laboratories found to be important for binding, we did not observe any complementary side chains that impact binding. In our studies, the Bcl-x_L/Mcl-1 residues with side chains that contact F18 in the crystal structure, F97 and Y101 in the case of

DOI: 10.1021/bi501505y
Biochemistry 2015, 54, 2632−2643

Bim and Y195 for Bak, showed only a small loss of signal when mutated. In order to exclude the possibility that attachment of the C-terminus of the helices to NF perturbs the interaction, we also tested a variant of Bim where the C-terminus of the helix was extended by four residues (Bim(l)-NF, Table S2), but no significant changes in binding were observed (data not shown). For both Bcl-x_L and Mcl-1, the Bim F18 residues makes several contacts that cannot be directly addressed by an alanine scan. For example, A93 and G138 for Bcl-x_L/Bim and A200 and the backbone of F97 in the case of Bcl-x_L:Bak cannot be interrogated by alanine substitutions. As a result, the observed lack of perturbation in binding may either be a case for distributed binding where several simultaneous mutations in the receptor would be required, or alternatively, this interaction may potentially be a result of the structure of the backbone alongside Ala and Gly contacts, akin to a knob and hole.

The only previous comprehensive experimental study focusing upon the receptor rather than the helices adapted a yeast display based selection approach.[17] This study interrogated the specificity of the BH3 helices Bad and Bim for various Bcl-x_L mutants, many of which were similar between our two panels. It should be noted that, as these residues were all covaried in this panel and there were many potential outputs as well as unique residue sets at each position, the results are not fully comparable. Even with this caveat, however, our results strongly correlate. For example, F97 was found to be essential for binding of Bcl-x_L to Bad but not Bim, consistent with our results. Surprisingly, they found that mutation of V126 or F146 to alanine increased binding to Bad over Bim, which is recapitulated in our study. Additionally, the Q111 position was shown to be nonspecific, which comports with our results that show that neither Bad nor Bim binding is affected by mutation (Figure 3). Overall, the data from our study provide a distinct and complementary picture of the important receptor residues corresponding to residues on the BH3 helices, which should allow for testing computational models and aid in targeting or redesigning relevant sites at these interfaces.

CONCLUSIONS

We have generated a receptor-centric interaction map of 23 helix/receptor pairs. Twelve alanine mutants of the three receptors, Bcl-x_L, Bcl-2, and Mcl-1, were interrogated against BH3 helices derived from Bid, Bim, Bad, Bik, Bmf, Bak, Hrk, and Puma using a split-luciferase method in cell lysates. This approach allows for the faithful identification of residues implicated in binding in complex cell lysates as evidenced by its strong correlation to previous experimental studies. We note that this method is qualitative and does not provide quantitative thermodynamic data; however, the results allow for the identification of the most important side-chains that contribute to binding. Moreover, we can match the residues that were found to dictate specificity and affinity of the helical BH3 domains with residues that line the complementary receptor cleft by a comparison of the two data sets, where available. Several notable observations were made. Only four residues (V220, N260, R263, and F319) in Mcl-1 primarily confer binding to all the helices tested, whereas the residues that contribute to binding for Bcl-2 and Bcl-x_L are distributed across the interface and are generally BH3 helix specific rather than conserved. Despite similar binding profiles among helices,[29−32] Bcl-x_L and Bcl-2 show distinct differences in the important residues for binding of several helices such as Puma (F97, E129, L130, N136, and R139 in Bcl-x_L, vs R146 and F153 in Bcl-2) and Bmf (F97, V126, L130, and R139 in Bcl-x_L vs Y108, L137, R146 and F153 in Bcl-2). In general, the receptors are possibly optimized for promiscuity, which is encoded in the structure by allowing variable modes of recognition for different BH3 helices. This may have functional consequences such as the ability to respond to a variety of signals or built-in functional redundancy. Finally, we determined that the conserved D16 residue on the helices is most likely recognized by both the conserved N136 as well as R139 on the receptors. Surprisingly, R139, thought to be essential for binding to all BH3 helices, was found to be dispensable for Bcl-x_L:Bad and when interrogated biophysically, we found that it recapitulated our observations from the split-luciferase assay, which may also have functional reasons. Future studies will probe the whether there is a biological rationale for why R139A is uniquely unimportant for Bcl-x_L:Bad binding compared to all other complexes. The R139A mutant also provides a starting point for creating potentially specific and orthogonal helix/receptor pairs for a variety of biotechnological studies[127−129] as well as the elucidation of the role in binding of the unique serine phosphorylation at this site.

We observed that the computational derived alanine mutation energies from Robetta and Rosetta that rely on analysis of existing structural data, as well as more dedicated molecular dynamics simulations, did not correlate well with the experimental data. A new computational approach reported by Keating and co-workers may be more suitable.[53,54] Given the inability for the more readily available methods to predict experimental results within this interactome, and their reliance on potentially sparse X-ray and NMR structures of interfaces, higher throughput direct experimental methods provide an avenue for understanding of factors that govern specificity and promiscuity at these interfaces.[23,107,130]

In the long term, the development of easy to implement experimental and computational methods in tandem are necessary for providing better predictive power to understand protein−protein interactions. This in turn will guide the knowledge based design of specific or selectively promiscuous inhibitors and provide guidelines for redesigned protein−protein interfaces for controlling cellular networks.

ASSOCIATED CONTENT

Supporting Information

Complex distance data, helix mutation data, list of constructs, full relative luminescence and standard deviation tables, 3D graphs of luminescence data, discussion of binding reductions, computational and experimental correlations, FPLC data, CD spectra, peptide synthesis details, HPLC data, and mass spectrum of peptide. This material is available free of charge via the Internet at http://pubs.acs.org.

AUTHOR INFORMATION

Corresponding Author

*E-mail: ghosh@email.arizona.edu.

Notes

The authors declare no competing financial interest.

ACKNOWLEDGMENTS

We thank members of the Ghosh lab and Dr. Reena Zutshi for helpful comments. We thank Professor Paramjit Arora and Andrew Watkins for helpful comments and assistance in implementing Rosetta.

DOI: 10.1021/bi501505y
Biochemistry 2015, 54, 2632−2643

■ ABBREVIATIONS

BH, Bcl-2 homology; PPI, protein−protein interactions; NF, N-terminal firefly luciferase; CF, C-terminal firefly luciferase; WT, wild type; CD, circular dichroism; ITC, isothermal titration calorimetry

■ REFERENCES

(1) Clackson, T., and Wells, J. A. (1995) A hot-spot of binding energy in a hormone-receptor interface. *Science 267*, 383−386.

(2) Bogan, A. A., and Thorn, K. S. (1998) Anatomy of hot spots in protein interfaces. *J. Mol. Biol. 280*, 1−9.

(3) DeLano, W. L. (2002) Unraveling hot spots in binding interfaces: progress and challenges. *Curr. Opin. Struct. Biol. 12*, 14−20.

(4) Wells, J. A. (1991) Systematic mutational analysis of protein interfaces. *Methods Enzymol. 202*, 390−411.

(5) Morrison, K. L., and Weiss, G. A. (2001) Combinatorial alanine-scanning. *Curr. Opin. Chem. Biol. 5*, 302−307.

(6) Sidhu, S. S., and Kossiakoff, A. A. (2007) Exploring and designing protein function with restricted diversity. *Curr. Opin. Chem. Biol. 11*, 347−354.

(7) Phillips, K. J., Rosenbaum, D. M., and Liu, D. R. (2006) Binding and stability determinants of the PPAR gamma nuclear receptor-coactivator interface as revealed by shotgun alanine scanning and in vivo selection. *J. Am. Chem. Soc. 128*, 11298−11306.

(8) Schreiber, G., and Keating, A. E. (2011) Protein binding specificity versus promiscuity. *Curr. Opin. Chem. Biol. 21*, 50−61.

(9) Keskin, O., Gursoy, A., Ma, B., and Nussinov, R. (2008) Principles of protein-protein interactions: What are the preferred ways for proteins to interact? *Chem. Rev. 108*, 1225−1244.

(10) Pawson, T., and Nash, P. (2003) Assembly of cell regulatory systems through protein interaction domains. *Science 300*, 445−452.

(11) Jacob, F. (1977) Evolution and tinkering. *Science 196*, 1161−1166.

(12) Pelletier, J. N., Arndt, K. M., Pluckthun, A., and Michnick, S. W. (1999) An in vivo library-versus-library selection of optimized protein-protein interactions. *Nat. Biotechnol. 17*, 683−690.

(13) Park, S. H., Zarrinpar, A., and Lim, W. A. (2003) Rewiring MAP kinase pathways using alternative scaffold assembly mechanisms. *Science 299*, 1061−1064.

(14) Howard, P. L., Chia, M. C., Del Rizzo, S., Liu, F. F., and Pawson, T. (2003) Redirecting tyrosine kinase signaling to an apoptotic caspase pathway through chimeric adaptor proteins. *Proc. Natl. Acac. Sci. U.S.A. 100*, 11267−11272.

(15) Dreze, M., Charloteaux, B., Milstein, S., Vidalain, P. O., Yildirim, M. A., Zhong, Q., Svrzikapa, N., Romero, V., Laloux, G., Brasseur, R., Vandenhaute, J., Boxem, M., Cusick, M. E., Hill, D. E., and Vidal, M. (2009) 'Edgetic' perturbation of a C. elegans BCL2 ortholog. *Nat. Methods 6*, 843−849.

(16) Dutta, S., Gulla, S., Chen, T. S., Fire, E., Grant, R. A., and Keating, A. E. (2010) Determinants of BH3 binding specificity for Mcl-1 versus BcI-x(L). *J. Mol. Biol. 398*, 747−762.

(17) Chen, T. S., Palacios, H., and Keating, A. E. (2013) Structure-based redesign of the binding specificity of anti-apoptotic Bcl-x_L. *J. Mol. Biol. 425*, 171−185.

(18) Chen, T. S., and Keating, A. E. (2012) Designing specific protein-protein interactions using computation, experimental library screening, or integrated methods. *Protein Sci. 21*, 949−963.

(19) Lim, W. A., Lee, C. M., and Tang, C. (2013) Design principles of regulatory networks: searching for the molecular algorithms of the cell. *Mol. Cell 49*, 202−212.

(20) Procko, E., Berguig, G. Y., Shen, B. W., Song, Y., Frayo, S., Convertine, A. J., Margineantu, D., Booth, G., Correia, B. E., Cheng, Y., Schief, W. R., Hockenbery, D. M., Press, O. W., Stoddard, B. L., Stayton, P. S., and Baker, D. (2014) A computationally designed inhibitor of an epstein-barr viral bcl-2 protein induces apoptosis in infected cells. *Cell 157*, 1644−1656.

(21) Goreshnik, I., and Maly, D. J. (2010) A small molecule-regulated guanine nucleotide exchange factor. *J. Am. Chem. Soc. 132*, 938−940.

(22) Kortemme, T., and Baker, D. (2004) Computational design of protein-protein interactions. *Curr. Opin. Chem. Biol. 8*, 91−97.

(23) Magliery, T. J., Wilson, C. G. M., Pan, W. L., Mishler, D., Ghosh, I., Hamilton, A. D., and Regan, L. (2005) Detecting protein-protein interactions with a green fluorescent protein fragment reassembly trap: Scope and mechanism. *J. Am. Chem. Soc. 127*, 146−157.

(24) Tsujimoto, Y., Cossman, J., Jaffe, E., and Croce, C. M. (1985) Involvement of the Bcl-2 gene in human follicular lymphoma. *Science 228*, 1440−1443.

(25) Hockenbery, D., Nunez, G., Milliman, C., Schreiber, R. D., and Korsmeyer, S. J. (1990) Bcl-2 is an inner mitochondrial-membrane protein that blocks programmed cell death. *Nature 348*, 334−336.

(26) Boise, L. H., Gonzalez-Garcia, M., Postema, C. E., Ding, L., Lindsten, T., Turka, L. A., Mao, X., Nunez, G., and Thompson, C. B. (1993) Bcl-x, a Bcl-2-related gene that functions as a dominant regulator of apoptotic regulator of apoptotic cell-death. *Cell 74*, 597−608.

(27) Yang, E., Zha, J., Jockel, J., Boise, L. H., Thompson, C. B., and Korsmeyer, S. J. (1995) Bad, a heterodimeric partner for Bcl-x_L and Bcl-2, displaces Bax and promtes cell-death. *Cell 80*, 285−291.

(28) Youle, R. J., and Strasser, A. (2008) The BCL-2 protein family: opposing activities that mediate cell death. *Nat. Rev. Mol. Cell Biol. 9*, 47−59.

(29) Chen, L., Willis, S. N., Wei, A., Smith, B. J., Fletcher, J. I., Hinds, M. G., Colman, P. M., Day, C. L., Adams, J. M., and Huang, D. C. S. (2005) Differential targeting of prosurvival Bcl-2 proteins by their BH3-only ligands allows complementary apoptotic function. *Mol. Cell 17*, 393−403.

(30) Letai, A., Bassik, M. C., Walensky, L. D., Sorcinelli, M. D., Weiler, S., and Korsmeyer, S. J. (2002) Distinct BH3 domains either sensitize or activate mitochondrial apoptosis, serving as prototype cancer therapeutics. *Cancer Cell 2*, 183−192.

(31) Certo, M., Moore, V. D. G., Nishino, M., Wei, G., Korsmeyer, S., Armstrong, S. A., and Letai, A. (2006) Mitochondria primed by death signals determine cellular addiction to antiapoptotic BCL-2 family members. *Cancer Cell 9*, 351−365.

(32) Ku, B., Liang, C., Jung, J. U., and Oh, B. H. (2011) Evidence that inhibition of BAX activation by BCL-2 involves its tight and preferential interaction with the BH3 domain of BAX. *Cell Res. 21*, 627−641.

(33) Wang, K., Yin, X., Chao, D. T., Milliman, C. L., and Korsmeyer, S. J. (1996) BID: A novel BH3 domain-only death agonist. *Genes Dev. 10*, 2859−2869.

(34) Wei, M. C., Zong, W. X., Cheng, E. H. Y., Lindsten, T., Panoutsakopoulou, V., Ross, A. J., Roth, K. A., MacCregor, G. R., Thompson, C. B., and Korsmeyer, S. J. (2001) Proapoptotic BAX and BAK: A requisite gateway to mitochondrial dysfunction and death. *Science 292*, 727−730.

(35) Kuwana, T., Mackey, M. R., Perkins, G., Ellisman, M. H., Latterich, M., Schneiter, R., Green, D. R., and Newmeyer, D. D. (2002) Bid, Bax, and lipids cooperate to form supramolecular openings in the outer mitochondrial membrane. *Cell 111*, 331−342.

(36) Kuwana, T., Bouchier-Hayes, L., Chipuk, J. E., Bonzon, C., Sullivan, B. A., Green, D. R., and Newmeyer, D. D. (2005) BH3 domains of BH3-only proteins differentially regulate bax-mediated mitochondrial membrane permeabilization both directly and indirectly. *Mol. Cell 17*, 525−535.

(37) Willis, S. N., Fletcher, J. I., Kaufmann, T., van Delft, M. F., Chen, L., Czabotar, P. E., Ierino, H., Lee, E. F., Fairlie, W. D., Bouillet, P., Strasser, A., Kluck, R. M., Adams, J. M., and Huang, D. C. S. (2007) Apoptosis initiated when BH3 ligands engage multiple Bcl-2 homologs, not Bax or Bak. *Science 315*, 856−859.

(38) Dai, H., Pang, Y. P., Ramirez-Alvarado, M., and Kaufmann, S. H. (2014) Evaluation of the BH3-only protein Puma as a direct Bak activator. *J. Biol. Chem. 289*, 89−99.

(39) Chipuk, J. E., Kuwana, T., Bouchier-Hayes, L., Droin, N. M., Newmeyer, D. D., Schuler, M., and Green, D. R. (2004) Direct activation of Bax by p53 mediates mitochondrial membrane permeabilization and apoptosis. *Science 303*, 1010−1014.

DOI: 10.1021/bi501505y
Biochemistry 2015, 54, 2632−2643

(40) Mahajan, I. M., Chen, M. D., Muro, I., Robertson, J. D., Wright, C. W., and Bratton, S. B. (2014) BH3-Only protein BIM mediates heat shock-induced apoptosis. *PLoS One 9*, No. e84388.
(41) Gavathiotis, E., Suzuki, M., Davis, M. L., Pitter, K., Bird, G. H., Katz, S. G., Tu, H. C., Kim, H., Cheng, E. H. Y., Tjandra, N., and Walensky, L. D. (2008) BAX activation is initiated at a novel interaction site. *Nature 455*, 1076−1081.
(42) Youle, R. J., and Karbowski, M. (2005) Mitochondrial fission in apoptosis. *Nat. Rev. Mol. Cell Biol. 6*, 657−663.
(43) Karbowski, M., Norris, K. L., Cleland, M. M., Jeong, S. Y., and Youle, R. J. (2006) Role of Bax and Bak in mitochondrial morphogenesis. *Nature 443*, 658−662.
(44) Autret, A., and Martin, S. J. (2009) Emerging role for members of the Bcl-2 family in mitochondrial morphogenesis. *Mol. Cell 36*, 355−363.
(45) Billen, L. P., Kokoski, C. L., Lovell, J. F., Leber, B., and Andrews, D. W. (2008) Bcl-XL inhibits membrane permeabilization by competing with Bax. *PLoS Biol. 6*, 1268−1280.
(46) Czabotar, P. E., Westphal, D., Dewson, G., Ma, S., Hockings, C., Fairlie, W. D., Lee, E. F., Yao, S., Robin, A. Y., Smith, B. J., Huang, D. C. S., Kluck, R. M., Adams, J. M., and Colman, P. M. (2013) Bax crystal structures reveal how BH3 domains activate Bax and nucleate its oligomerization to induce apoptosis. *Cell 152*, 519−531.
(47) Happo, L., Strasser, A., and Cory, S. (2012) BH3-only proteins in apoptosis at a glance. *J. Cell Sci. 125*, 1081−1087.
(48) Goreshnik, I., Brock, A. M., and Maly, D. J. (2011) Biochemical and pharmacological profiling of the pro-survival protein Bcl-xL. *Bioorg. Med. Chem. Lett. 21*, 4951−4955.
(49) Cheng, E. H. Y., Levine, B., Boise, L. E., Thompson, C. B., and Hardwick, J. M. (1996) Bax-independent inhibition of apoptosis by Bcl-x_L. *Nature 379*, 554−556.
(50) Petros, A. M., Nettesheim, D. G., Wang, Y., Olejniczak, E. T., Meadows, R. P., Mack, J., Swift, K., Matayoshi, E. D., Zhang, H., Thompson, C. B., and Fesik, S. W. (2000) Rationale for Bcl-x_L/Bad peptide complex formation from structure, mutagenesis, and biophysical studies. *Protein Sci. 9*, 2528−2534.
(51) Sattler, M., Liang, H., Nettesheim, D., Meadows, R. P., Harlan, J., Eberstadt, M., Yoon, H. S., Shuker, S. B., Chang, B. S., Minn, A. J., Thompson, C. B., and Fesik, S. W. (1997) Structure of Bcl-x_L-Bak peptide complex: Recognition between regulators of apoptosis. *Science 275*, 983−986.
(52) Boersma, M. D., Sadowsky, J. D., Tomita, Y. A., and Gellman, S. H. (2008) Hydrophile scanning as a complement to alanine scanning for exploring and manipulating protein-protein recognition: Application to the Bim BH3 domain. *Protein Sci. 17*, 1232−1240.
(53) DeBartolo, J., Dutta, S., Reich, L., and Keating, A. E. (2012) Predictive Bcl-2 family binding models rooted in experiment or structure. *J. Mol. Biol. 422*, 124−144.
(54) London, N., Gulla, S., Keating, A. E., and Schueler-Furman, O. (2012) In silico and in vitro elucidation of BH3 binding specificity toward Bcl-2. *Biochemistry 51*, 5841−5850.
(55) Vaux, D. L., Cory, S., and Adams, J. M. (1988) Bcl-2 gene promotes haemopoietic cell survival and cooperates with c-myc to immortalize pre-B cells. *Nature 335*, 440−442.
(56) Rampino, N., Yamamoto, H., Ionov, Y., Li, Y., Sawai, H., Reed, J. C., and Perucho, M. (1997) Somatic frameshift mutations in the BAX gene in colon cancers of the microsatellite mutator phenotype. *Science 275*, 967−969.
(57) Hanahan, D., and Weinberg, R. A. (2011) Hallmarks of cancer: The next generation. *Cell 144*, 646−674.
(58) Juin, P., Geneste, O., Gautier, F., Depil, S., and Campone, M. (2013) Decoding and unlocking the BCL-2 dependency of cancer cells. *Nat. Rev. Cancer 13*, 455−465.
(59) Fesik, S. W. (2005) Promoting apoptosis as a strategy for cancer drug discovery. *Nat. Rev. Cancer 5*, 876−885.
(60) Ardestani, A., Paroni, F., Azizi, Z., Kaur, S., Khobragade, V., Yuan, T., Frogne, T., Tao, W., Oberholzer, J., Pattou, F., Conte, J. K., and Maedler, K. (2014) MST1 is a key regulator of beta cell apoptosis and dysfunction in diabetes. *Nat. Med. 20*, 385−397.
(61) Degterev, A., Lugovskoy, A., Cardone, M., Mulley, B., Wagner, G., Mitchison, T., and Yuan, J. (2001) Identification of small-molecule inhibitors of interaction between the BH3 domain and Bcl-x_L. *Nat. Cell Biol. 3*, 173−182.
(62) Enyedy, I. J., Ling, Y., Nacro, K., Tomita, Y., Wu, X., Cao, Y., Guo, R., Li, B., Zhu, X., Huang, Y., Long, Y. Q., Roller, P. P., Yang, D., and Wang, S. (2001) Discovery of small-molecule inhibitors of Bcl-2 through structure-based computer screening. *J. Med. Chem. 44*, 4313−4324.
(63) Kutzki, O., Park, H. S., Ernst, J. T., Orner, B. P., Yin, H., and Hamilton, A. D. (2002) Development of a potent Bcl-x_L antagonist based on α-helix mimicry. *J. Am. Chem. Soc. 124*, 11838−11839.
(64) Ernst, J. T., Becerril, J., Park, H. S., Yin, H., and Hamilton, A. D. (2003) Design and application of an α-helix-mimetic scaffold based on an oligoamide-foldamer strategy: Antagonism of the bak BH3/Bcl-xL complex. *Angew. Chem., Int. Ed. 42*, 535−539.
(65) Oltersdorf, T., Elmore, S. W., Shoemaker, A. R., Armstrong, R. C., Augeri, D. J., Belli, B. A., Bruncko, M., Deckwerth, T. L., Dinges, J., Hajduk, P. J., Joseph, M. K., Kitada, S., Korsmeyer, S. J., Kunzer, A. R., Letai, A., Li, C., Mitten, M. J., Nettesheim, D. G., Ng, S., Nimmer, P. M., O'Connor, J. M., Oleksijew, A., Petros, A. M., Reed, J. C., Shen, W., Tahir, S. K., Thompson, C. B., Tomaselli, K. J., Wang, B., Wendt, M. D., Zhang, H., Fesik, S. W., and Rosenberg, S. H. (2005) An inhibitor of Bcl-2 family proteins induces regression of solid tumours. *Nature 435*, 677−681.
(66) Lee, E. F., Czabotar, P. E., Smith, B. J., Deshayes, K., Zobel, K., Colman, P. M., and Fairlie, W. D. (2007) Crystal structure of ABT-737 complexed with Bcl-xL: implications for selectivity of antagonists of the Bcl-2 family. *Cell Death Differ. 14*, 1711−1713.
(67) Park, C. M., Bruncko, M., Adickes, J., Bauch, J., Ding, H., Kunzer, A., Marsh, K. C., Nimmer, P., Shoemaker, A. R., Song, X., Tahir, S. K., Tse, C., Wang, X., Wendt, M. D., Yang, X., Zhang, H., Fesik, S. W., Rosenberg, S. H., and Elmore, S. W. (2008) Discovery of an orally bioavailable small molecule inhibitor of prosurvival B-cell lymphoma 2 proteins. *J. Med. Chem. 51*, 6902−6915.
(68) Porter, J. R., Helmers, M. R., Wang, P., Furman, J. L., Joy, S. T., Arora, P. S., and Ghosh, I. (2010) Profiling small molecule inhibitors against helix-receptor interactions: the Bcl-2 family inhibitor BH3I-1 potently inhibits p53/hDM2. *Chem. Commun. 46*, 8020−8022.
(69) Kazi, A., Sun, J., Doi, K., Sung, S. S., Takahashi, Y., Yin, H., Rodriguez, J. M., Becerril, J., Berndt, N., Hamilton, A. D., Wang, H. G., and Sebti, S. M. (2011) The BH3 α-helical mimic BH3-M6 disrupts Bcl-X_L, Bcl-2, and MCL-1 protein-protein interactions with Bax, Bak, Bad, or Bim and induces apoptosis in a Bax- and Bim-dependent manner. *J. Biol. Chem. 286*, 9382−9392.
(70) Lessene, G., Czabotar, P. E., Sleebs, B. E., Zobel, K., Lowes, K. N., Adams, J. M., Baell, J. B., Colman, P. M., Deshayes, K., Fairbrother, W. J., Flygare, J. A., Gibbons, P., Kersten, W. J. A., Kulasegaram, S., Moss, R. M., Parisot, J. P., Smith, B. J., Street, I. P., Yang, H., Huang, D. C. S., and Watson, K. G. (2013) Structure-guided design of a selective BCL-X_L inhibitor. *Nat. Chem. Biol. 9*, 390−397.
(71) Azzarito, V., Long, K., Murphy, N. S., and Wilson, A. J. (2013) Inhibition of α-helix-mediated protein-protein interactions using designed molecules. *Nat. Chem. 5*, 161−173.
(72) Tanaka, Y., Aikawa, K., Nishida, G., Homma, M., Sogabe, S., Igaki, S., Hayano, Y., Sameshima, T., Miyahisa, I., Kawamoto, T., Tawada, M., Imai, Y., Inazuka, M., Cho, N., Imaeda, Y., and Ishikawa, T. (2013) Discovery of potent Mcl-1/Bcl-xL dual inhibitors by using a hybridization strategy based on structural analysis of target proteins. *J. Med. Chem. 56*, 9635−9645.
(73) Souers, A. J., Leverson, J. D., Boghaert, E. R., Ackler, S. L., Catron, N. D., Chen, J., Dayton, B. D., Ding, H., Enschede, S. H., Fairbrother, W. J., Huang, D. C. S., Hymowitz, S. G., Jin, S., Khaw, S. L., Kovar, P. J., Lam, L. T., Lee, J., Maecker, H. L., Marsh, K. C., Mason, K. D., Mitten, M. J., Nimmer, P. M., Oleksijew, A., Park, C. H., Park, C. M., Phillips, D. C., Roberts, A. W., Sampath, D., Seymour, J. F., Smith, M. L., Sullivan, G. M., Tahir, S. K., Tse, C., Wendt, M. D., Xiao, Y., Xue, J. C., Zhang, H., Humerickhouse, R. A., Rosenberg, S. H., and Elmore, S. W. (2013) ABT-199, a potent and selective BCL-2

DOI: 10.1021/bi501505y
Biochemistry 2015, 54, 2632−2643

inhibitor, achieves antitumor activity while sparing platelets. *Nat. Med. 19*, 202−208.
(74) Fu, X., Apgar, J. R., and Keating, A. E. (2007) Modeling backbone flexibility to achieve sequence diversity: The design of novel alpha-helical ligands for Bcl-x_L. *J. Mol. Biol. 371*, 1099−1117.
(75) Stewart, M. L., Fire, E., Keating, A. E., and Walensky, L. D. (2010) The MCL-1 BH3 helix is an exclusive MCL-1 inhibitor and apoptosis sensitizer. *Nat. Chem. Biol. 6*, 595−601.
(76) Holinger, E. P., Chittenden, T., and Lutz, R. J. (1999) Bak BH3 peptides antagonize Bcl-x_L function and induce apoptosis through cytochrome c-independent activation of caspases. *J. Biol. Chem.*, 13298−13304.
(77) Chin, J. W., and Schepartz, A. (2001) Design and evolution of a miniature Bcl-2 binding protein. *Angew. Chem., Int. Ed. 40*, 3922−3925.
(78) Gemperli, A. C., Rutledge, S. E., Maranda, A., and Schepartz, A. (2005) Paralog-selective ligands for Bcl-2 proteins. *J. Am. Chem. Soc. 127*, 1596−1597.
(79) Schafmeister, C. E., Po, J., and Verdine, G. L. (2000) An all-hydrocarbon cross-linking system for enhancing the helicity and metabolic stability of peptides. *J. Am. Chem. Soc. 122*, 5891−5892.
(80) Walensky, L. D., Kung, A. L., Escher, I., Malia, T. J., Barbuto, S., Wright, R. D., Wagner, G., Verdine, G. L., and Korsmeyer, S. J. (2004) Activation of apoptosis in vivo by a hydrocarbon-stapled BH3 helix. *Science 305*, 1466−1470.
(81) Walensky, L. D., Pitter, K., Morash, J., Oh, K. J., Barbuto, S., Fisher, J., Smith, E., Verdine, G. L., and Korsmeyer, S. J. (2006) A stapled BID BH3 helix directly binds and activates BAX. *Mol. Cell 24*, 199−210.
(82) Okamoto, T., Zobel, K., Fedorova, A., Quan, C., Yang, H., Fairbrother, W. J., Huang, D. C. S., Smith, B. J., Deshayes, K., and Czabotar, P. E. (2013) Stabilizing the pro-apoptotic BimBH3 helix (BimSAHB) does not necessarily enhance affinity or biological activity. *ACS Chem. Biol. 8*, 297−302.
(83) Bird, G. H., Gavathiotis, E., LaBelle, J. L., Katz, S. G., and Walensky, L. D. (2014) Distinct BimBH3 (BimSAHB) stapled peptides for structural and cellular studies. *ACS Chem. Biol. 9*, 831−837.
(84) Wang, D., Liao, W., and Arora, P. S. (2005) Binding properties of artificial α helices derived from a hydrogen-bond surrogate: Application to Bcl-xL. *Angew. Chem., Int. Ed. 44*, 6525−6529.
(85) Henchey, L. K., Jochim, A. L., and Arora, P. S. (2008) Contemporary strategies for the stabilization of peptides in the α-helical conformation. *Curr. Opin. Chem. Biol. 12*, 692−697.
(86) Henchey, L. K., Porter, J. R., Ghosh, I., and Arora, P. S. (2010) High specificity in protein recognition by hydrogen-bond-surrogate α-helices: Selective inhibition of the p53/MDM2 complex. *ChemBioChem 11*, 2104−2107.
(87) Muppidi, A., Doi, K., Edwardraja, S., Drake, E. J., Gulick, A. M., Wang, H. G., and Lin, Q. (2012) Rational design of proteolytically stable, cell-permeable peptide-based selective Mcl-1 inhibitors. *J. Am. Chem. Soc. 134*, 14734−14737.
(88) Muppidi, A., Doi, K., Edwardraja, S., Pulayarti, S. V. S. R. K., Szyperski, T., Wang, H. G., and Lin, Q. (2014) Targeted delivery of ubiquitin-conjugated BH3 peptide-based Mcl-1 inhibitors into cancer cells. *Bioconjugate Chem. 25*, 424−432.
(89) Sadowsky, J. D., Schmitt, M. A., Lee, H. S., Umezawa, N., Wang, S., Tomita, Y., and Gellman, S. H. (2005) Chimeric (α/β+α)-peptide ligands for the BH3-recognition cleft of Bcl-x_L: Critical role of the molecular scaffold in protein surface recognition. *J. Am. Chem. Soc. 127*, 11966−11968.
(90) Sadowsky, J. D., Fairlie, W. D., Hadley, E. B., Lee, H. S., Umezawa, N., Nikolovska-Coleska, Z., Wang, S. M., Huang, D. C. S., Tomita, Y., and Gellman, S. H. (2007) α/β+α)-peptide antagonists of BH3 domain/Bcl-x_L recognition: Toward general strategies for foldamer-based inhibition of protein-protein interactions. *J. Am. Chem. Soc. 129*, 139−154.
(91) Sadowsky, J. D., Murray, J. K., Tomita, Y., and Gellman, S. H. (2007) Exploration of backbone space in foldamers containing α- and β-amino acid residues: Developing protease-resistant oligomers that bind tightly to the BH3-recognition cleft of Bcl-x_L. *ChemBioChem 8*, 903−916.
(92) Horne, W. S., Boersma, M. D., Windsor, M. A., and Gellman, S. H. (2008) Sequence-based design of α/β-peptide foldamers that mimic BH3 domains. *Angew. Chem., Int. Ed. 47*, 2853−2856.
(93) Lee, E. F., Sadowsky, J. D., Smith, B. J., Czabotar, P. E., Peterson-Kaufman, K. J., Colman, P. M., Gellman, S. H., and Fairlie, W. D. (2009) High-resolution structural characterization of a helical α/β-peptide foldamer bound to the anti-apoptotic protein Bcl-x_L. *Angew. Chem., Int. Ed. 48*, 4318−4322.
(94) Lee, E. F., Smith, B. J., Horne, W. S., Mayer, K. N., Evangelista, M., Colman, P. M., Gellman, S. H., and Fairlie, W. D. (2011) Structural basis of Bcl-x_L recognition by a BH3-mimetic α/β-peptide generated by sequence-based design. *ChemBioChem 12*, 2025−2032.
(95) Boersma, M. D., Haase, H. S., Peterson-Kaufman, K. J., Lee, E. F., Clarke, O. B., Colman, P. M., Smith, B. J., Horne, W. S., Fairlie, W. D., and Gellman, S. H. (2012) Evaluation of diverse α/β-backbone patterns for functional α-helix mimicry: Analogues of the Bim BH3 domain. *J. Am. Chem. Soc. 134*, 315−323.
(96) Smith, B. J., Lee, E. F., Checco, J. W., Evangelista, M., Gellman, S. H., and Fairlie, W. D. (2013) Structure-guided rational design of α/β-peptide foldamers with high affinity for BCL-2 family prosurvival proteins. *ChemBioChem 14*, 1564−1572.
(97) Liu, X., Dai, S., Zhu, Y., Marrack, P., and Kappler, J. W. (2003) The structure of a Bcl-x_L/Bim fragment complex: implications for bim function. *Immunity 19*, 341−352.
(98) Manion, M. K., O'Neill, J. W., Giedt, C. D., Kim, K. M., Zhang, K. Y. Z., and Hockenbery, D. M. (2004) Bcl-X_L mutations suppress cellular sensitivity to Antimycin A. *J. Biol. Chem. 279*, 2159−2165.
(99) Muchmore, S. W., Sattler, M., Liang, H., Meadows, R. P., Harlan, J. W., Yoon, H. S., Nettesheim, D., Chang, B. S., Thompson, C. B., Wong, S. L., Ng, S. C., and Fesik, S. W. (1996) X-ray and NMR structure of human Bcl-x_L, an inhibitor of programmed cell death. *Nature 381*, 335−341.
(100) Fire, E., Gulla, S. V., Grant, R. A., and Keating, A. E. (2010) Mcl-1-Bim complexes accommodate surprising point mutations via minor structural changes. *Protein Sci. 19*, 507−519.
(101) Lee, E. F., Czabotar, P. E., Yang, H., Sleebs, B. E., Lessene, G., Colman, P. M., Smith, B. J., and Fairlie, W. D. (2009) Conformational changes in Bcl-2 pro-survival proteins determine their capacity to bind ligands. *J. Biol. Chem. 284*, 30508−30517.
(102) Czabotar, P. E., Lee, E. F., Thompson, G. V., Wardak, A. Z., Fairlie, W. D., and Colman, P. M. (2011) Mutation to Bax beyond the BH3 domain disrupts interactions with pro-survival proteins and promotes apoptosis. *J. Biol. Chem. 286*, 7123−7131.
(103) Day, C. L., Smits, C., Fan, F. C., Lee, E. F., Fairlie, W. D., and Hinds, M. G. (2008) Structure of the BH3 domains from the p53-inducible BH3-only proteins Noxa and Puma in complex with Mcl-1. *J. Mol. Biol. 380*, 958−971.
(104) Priyadarshi, A., Roy, A., Kim, K. S., Kim, E. E., and Hwang, K. Y. (2010) Structural insights into mouse anti-apoptotic Bcl-xl reveal affinity for Beclin 1 and gossypol. *Biochem. Biophys. Res. Commun. 394*, 515−521.
(105) Lama, D., and Sankararamakrishnan, R. (2008) Anti-apoptotic Bcl-X_L protein in complex with BH3 peptides of pro-apoptotic Bak, Bad, and Bim proteins: Comparative molecular dynamics simulations. *Proteins: Struct., Funct., Bioinf. 73*, 492−514.
(106) Moroy, G., Martin, E., Dejaegere, A., and Stote, R. H. (2009) Molecular basis for Bcl-2 homology 3 domain recognition in the Bcl-2 protein family: identification of conserved hot-spot interactions. *J. Biol. Chem. 284*, 17499−17511.
(107) Porter, J. R., Stains, C. I., Jester, B. W., and Ghosh, I. (2008) A general and rapid cell-free approach for the interrogation of protein-protein, protein-DNA, and protein-RNA interactions and their antagonists utilizing split-protein reporters. *J. Am. Chem. Soc. 130*, 6488−6497.
(108) Luker, K. E., Smith, M. C. P., Luker, G. D., Gammon, S. T., Piwnica-Worms, H., and Piwnica-Worms, D. (2004) Kinetics of regulated protein-protein interactions revealed with firefly luciferase

DOI: 10.1021/bi501505y
Biochemistry 2015, 54, 2632−2643

complementation imaging in cells and living animals. *Proc. Natl. Acad. Sci. U.S.A. 101*, 12288−12293.
(109) Shekhawat, S. S., and Ghosh, I. (2011) Split-protein systems: Beyond binary protein-protein interactions. *Curr. Opin. Chem. Biol. 15*, 789−797.
(110) Paulmurugan, R., and Gambhir, S. S. (2005) Firefly luciferase enzyme fragment complementation for imaging in cells and living animals. *Anal. Chem. 77*, 1295−1302.
(111) Fields, S., and Song, O. K. (1989) A novel genetic system to detect protein protein interactions. *Nature 340*, 245−246.
(112) Phizicky, E., Bastiaens, P. I. H., Zhu, H., Snyder, M., and Fields, S. (2003) Protein analysis on a proteomic scale. *Nature 422*, 208−215.
(113) Sprinzak, E., Sattath, S., and Margalit, H. (2003) How reliable are experimental protein-protein interaction data? *J. Mol. Biol. 327*, 919−923.
(114) Kortemme, T., Kim, D. E., and Baker, D. (2004) Computational alanine scanning of protein-protein interfaces. *Sci. STKE 2004*, pl2.
(115) Kortemme, T., and Baker, D. (2002) A simple physical model for binding energy hot spots in protein-protein complexes. *Proc. Natl. Acac. Sci. U.S.A. 99*, 14116−14121.
(116) Das, R., and Baker, D. (2008) Macromolecular modeling with Rosetta. *Annu. Rev. Biochem. 77*, 363−382.
(117) Keeble, A. H., Joachimiak, L. A., Mate, M. J., Meenan, N., Kirkpatrick, N., Baker, D., and Kleanthous, C. J. (2008) Experimental and computational analyses of the energetic basis for dual recognition of immunity proteins by colicin endonucleases. *J. Mol. Biol. 379*, 745−759.
(118) Meenan, N. A. G., Sharma, A., Fleishman, S. J., MacDonald, C. J., Morel, B., Boetzel, R., Moore, G. R., Baker, D., and Kleanthous, C. (2010) The structural and energetic basis for high selectivity in a high-affinity protein-protein interaction. *Proc. Natl. Acac. Sci. U.S.A.*, 10080−10085.
(119) Zhou, X. M., Liu, Y., Payne, G., Lutz, R. J., and Chittenden, T. (2000) Growth factors inactivate the cell death promoter BAD by phosphorylation of its BH3 domain on Ser155. *J. Biol. Chem. 275*, 25046−25051.
(120) Datta, S. R., Katsov, A., Hu, L., Petros, A., Fesik, S. W., Yaffe, M. B., and Greenberg, M. E. (2000) 14−3-3 proteins and survival kinases cooperate to inactivate BAD by BH3 domain phosphorylation. *Mol. Cell 6*, 41−51.
(121) Datta, S. R., Dudek, H., Tao, X., Masters, S., Fu, H., Gotoh, Y., and Greenberg, M. E. (1997) Akt phosphorylation of BAD couples survival signals to the cell-intrinsic death machinery. *Cell 91*, 231−241.
(122) Chen, Y. H., Yang, J. T., and Chau, K. H. (1974) Determination of the helix and β form of proteins in aqueous solution by circular dichroism. *Biochemistry 13*, 3350−3359.
(123) Greenfield, N., and Fasman, G. D. (1969) Computed circular dichroism spectra for the evaluation of protein conformation. *Biochemistry 8*, 4108−4116.
(124) Thuduppathy, G. R., and Hill, R. B. (2006) Acid destabilization of the solution conformation of Bcl-X_L does not drive its pH-dependent insertion into membranes. *Protein Sci. 15*, 248−257.
(125) Xie, Z., Schendel, S., Matsuyama, S., and Reed, J. C. (1998) Acidic pH promotes dimerization of Bcl-2 family proteins. *Biochemistry 37*, 6410−6418.
(126) Leavitt, S., and Freire, E. (2001) Direct measurement of protein binding energetics by isothermal titration calorimetry. *Curr. Opin. Struct. Biol. 11*, 560−566.
(127) Shekhawat, S. S., Campbell, S. T., and Ghosh, I. (2011) A comprehensive panel of turn-on caspase biosensors for investigating caspase specificity and caspase activation pathways. *ChemBioChem 12*, 2353−2364.
(128) Shekhawat, S. S., Porter, J. R., Sriprasad, A., and Ghosh, I. (2009) An autoinhibited coiled-coil design strategy for split-protein protease sensors. *J. Am. Chem. Soc. 131*, 15284−15290.
(129) Boyle, A. L., and Woolfson, D. N. (2011) De novo designed peptides for biological applications. *Chem. Soc. Rev. 40*, 4295−4306.
(130) Lavinder, J. J., Hari, S. B., Sullivan, B. J., and Magliery, T. J. (2009) High-throughput thermal scanning: A general, rapid dye-binding thermal shift screen for protein engineering. *J. Am. Chem. Soc. 131*, 3794−3795.

DOI: 10.1021/bi501505y
Biochemistry 2015, 54, 2632−2643